

Bulk photovoltaic effect modulated by ferroelectric polarization back-switching

Cite as: Appl. Phys. Lett. **120**, 242901 (2022); <https://doi.org/10.1063/5.0094837>

Submitted: 06 April 2022 • Accepted: 27 May 2022 • Published Online: 13 June 2022

 Yunwei Sheng,  Ignasi Fina, Marin Gospodinov, et al.



View Online



Export Citation



CrossMark

 QBLOX



1 qubit

Shorten Setup Time

Auto-Calibration

More Qubits

Fully-integrated

Quantum Control Stacks

Ultrastable DC to 18.5 GHz

Synchronized <<1 ns

Ultralow noise



100s qubits

visit our website >

Bulk photovoltaic effect modulated by ferroelectric polarization back-switching

Cite as: Appl. Phys. Lett. **120**, 242901 (2022); doi: [10.1063/5.0094837](https://doi.org/10.1063/5.0094837)

Submitted: 6 April 2022 · Accepted: 27 May 2022 ·

Published Online: 13 June 2022



View Online



Export Citation



CrossMark

Yunwei Sheng,¹ Ignasi Fina,¹ Marin Gospodinov,² and Josep Fontcuberta^{1,a)}

AFFILIATIONS

¹Institut de Ciència de Materials de Barcelona (ICMAB-CSIC), Campus UAB, Bellaterra 08193, Catalonia, Spain

²Institute of Solid State Physics, Bulgarian Academy of Sciences, 1784 Sofia, Bulgaria

^{a)}Author to whom correspondence should be addressed: fontcuberta@icmab.cat

ABSTRACT

Short-circuit photocurrent due to bulk photovoltaic effect displays an oscillatory dependence on the polarization state of light. Here, we explore how the ferroelectric polarization direction in h -LuMnO₃ crystals affects the oscillating short-circuit photocurrent. It is shown that after prepoling the crystal at saturation, at remanence, the direction and amplitude of photocurrent oscillations are no longer dictated by prepoling voltage but are largely modulated by polarization back-switching, here ruled by the imprint field. Thus, the light polarization dependence of photocurrent is also ruled by the imprint field. The impact of these effects on the determination of the Glass coefficients of the material is discussed.

© 2022 Author(s). All article content, except where otherwise noted, is licensed under a Creative Commons Attribution (CC BY) license (<http://creativecommons.org/licenses/by/4.0/>). <https://doi.org/10.1063/5.0094837>

Bulk photovoltaic effect (BPE) occurs in non-centrosymmetric materials.^{1–4} In recent years, interest on BPE has been renewed mainly because the open circuit voltage is not limited by the bandgap of the absorber, but can be orders of magnitude larger.⁵ BPE is governed by optically induced excitations between ground and excited states, most commonly assumed to be the valence and conduction bands, although the contribution of in-gap states to BPE has been reported.⁶ The BPE photocurrent under illumination of a linearly polarized light is given by $J_{\text{BPE},i} \approx G_{ijk} e_j e_k$, where $J_{\text{BPE},i}$ denotes the BPE photocurrent density measured along the i direction and e_{jk} are the light polarization components along the j and k directions.⁷ The symmetry of the Glass tensor $\{G_{ijk}\}$ collects the point symmetry of the studied material,⁸ and the values of its elements which depend on photon energy, are dictated by specific features of the electronic band structure.⁹ As a result, there is a genuine dependence of short circuit current density (J_{sc}) on polarization of the incoming photons.

Determination of the G_{ijk} elements involves measuring J_{sc} along different directions (i, j, k) when the sample is illuminated with light of a given wavelength (λ) at different incidence angles (θ) with respect to the normal to sample surface and different polarization angles (φ). Typically, oscillating $J_{\text{sc}}(\theta, \varphi)$ behavior is observed, whose details depend on the symmetry-related structure, illumination configuration, and the values of the G_{ijk} elements.

When measuring J_{sc} in ferroelectric materials, several contributions may exist and be entangled. Other than J_{BPE} , drift photocurrent (J_{E}) arising from internal fields of various sources [i.e., Schottky (E_{bi}), depoling (E_{dep}), imprint (E_{im}), etc.] and a diffusion term (J_{D}) associated with photoinduced charge gradients may coexist and contribute to the measured J_{sc} .^{10,11} Discerning these different contributions to J_{sc} ($=J_{\text{BPE}} + J_{\text{E}} + J_{\text{D}}$), particularly J_{BPE} and J_{E} , requires knowing the ferroelectric polarization \mathbf{P} state when J_{sc} is measured.¹² This seemingly simple requirement, in practice, could be difficult to achieve. Indeed, the presence of E_{dep} and E_{im} may hinder, keeping the polarization at saturated state,^{13,14} and at remanence, when J_{sc} is measured, polarization back-switching may have occurred leading to a ferroelectric multidomain state or even reversing the overall polarization.¹⁵ As reversing the ferroelectric \mathbf{P} is equivalent to a spatial inversion, J_{BPE} should change its sign with equal magnitude because the $\{G_{ijk}\}$ tensor is odd (see details in the [supplementary material](#), S1).^{8,16,17} Similarly, J_{E} can be changed upon reversing \mathbf{P} as the depoling field/Schottky barriers are modulated.^{18,19} Therefore, the amplitude of the observed J_{BPE} oscillations may not be as expected for a fully polarized sample. Moreover, in general, at oblique incidence, the intensity of light transmitted and reflected at any interface should also depend on the polarization state (π or σ) of the incoming light (Fresnel coefficients), thus producing a modulation of J_{sc} ^{20,21} irrespectively of the origin of the photocurrent.

Here, we address this issue by measuring J_{sc} in uniaxial ferroelectric single crystals. Hexagonal h -LuMnO₃ is a room-temperature narrow-gap ferroelectric,^{22,23} where the polarization axis is along the hexagonal c -axis, either pointing up or down. It will be shown that the J_{sc} magnitude and its dependence on light polarization $J_{sc}(\varphi)$ are largely affected by the back-switching effect. More precisely, imprint governs the back-switching as evidenced by polarization retention measurements, performed on crystals displaying opposite imprint directions, which translates into the amplitude of $J_{sc}(\varphi)$. Consequently, the quantitative extraction of the Glass coefficients can be severely hampered.

We report data on two single crystals (I and II) of h -LuMnO₃ (LMO) around 100 μm thick with its hexagonal c -axis along the perpendicular to the largest surface. Crystals I and II were selected to display opposite imprint direction (see below). Pt contacts were deposited on top of the crystals (Pt_{top}, 7 nm thick, with transparency at 405 nm around 50%) forming capacitor structures labeled as E_n ($n = 1, 2, 3, \dots$).²⁴ The bottom side of the crystals was fully covered by continuous Pt contact (Pt_{bot}, 7 nm thick). Details on experiments are included in the [supplementary material](#), S2.

Figure 1(a) depicts the $I(V)$ curves recorded on illustrative capacitors (E₁, E₂, and E₃) on crystal-I. Data show obvious current peaks indicating polarization switching at coercive voltages (V_c^+ and V_c^-). The polarization $P(V)$ loops are shown in Fig. 1(b). The saturation polarization is about 9 $\mu\text{C}/\text{cm}^2$, which is somewhat larger than typically found in hexagonal manganites.^{18,25,26} Of interest here is that the I - V loops clearly reflect an imprint field (loops are shifted toward negative voltages), which indicates the presence of an internal field pointing downward [Fig. 1(c)]. From Fig. 1(b), we obtain $E_{im} [= (V_c^+ + V_c^-)/2]$ of -2.22 V, -3.21 V, and -4.26 V for E₁, E₂, and E₃,

respectively. It is worth noticing that the loops in Figs. 1(a) and 1(b) have been collected at 1 kHz without delay time.

The short-circuit photocurrent along the hexagonal axis is monitored while rotating the light polarization angle φ , with an incidence angle of $\theta \approx 45^\circ$ [Fig. 1(c)]. Data corresponding to electrode E₁ [Fig. 1(d)] have been collected after prepoling the sample with $V^{+/-} = \pm 60$ V. We first note in Fig. 1(d) the characteristic oscillations of $J_{sc}(\varphi)$ that are typically but disputably taken as fingerprints of BPE. Data can be fitted using the following equation, as predicted by the BPE theory:^{8,27,28}

$$J_{sc}(\varphi) = A_z \cos 2(\varphi + \varphi_0) + B_z, \quad (1)$$

where the subindex z signals that photocurrent is measured along z -axis (out of plane), and φ_0 ($\leq 5^\circ$) is a phase shift related to experimental uncertainties. Data in Fig. 1(d) also evidence a dependence of background current [$B_z(V^+) > B_z(V^-)$] and of amplitude (A_z) of the $J_{sc}(\varphi)$ oscillations on the sign of the voltage $V^{+/-}$ used to write the capacitor. The amplitude variation [$A_z(V^+) > A_z(V^-)$] can be better appreciated in Fig. 1(e) where data have been vertically shifted to match at $\varphi = 90^\circ$. In Fig. 1(f), we show the J_{sc} recorded in three capacitors after prepoling with V^+ . Clearly, the background current and the amplitude of oscillations vary similarly among electrodes but with $A_z/B_z \approx 0.1$ almost constant among various capacitors.

In Fig. 1(d), the sign of J_{sc} is independent of the sign (+/-) of the prepoling voltage. We notice that the observed E_{im} , evident in the $I(V)$ and $P(V)$ loops in Figs. 1(a) and 1(b), may have promoted a fast-preferential back-switching of the polarization before J_{sc} is recorded. We remark recording that the whole $J_{sc}(\varphi)$ [Figs. 1(d)–1(f)] sweep takes $\tau \approx 162$ s, which may be much longer than the required polarization

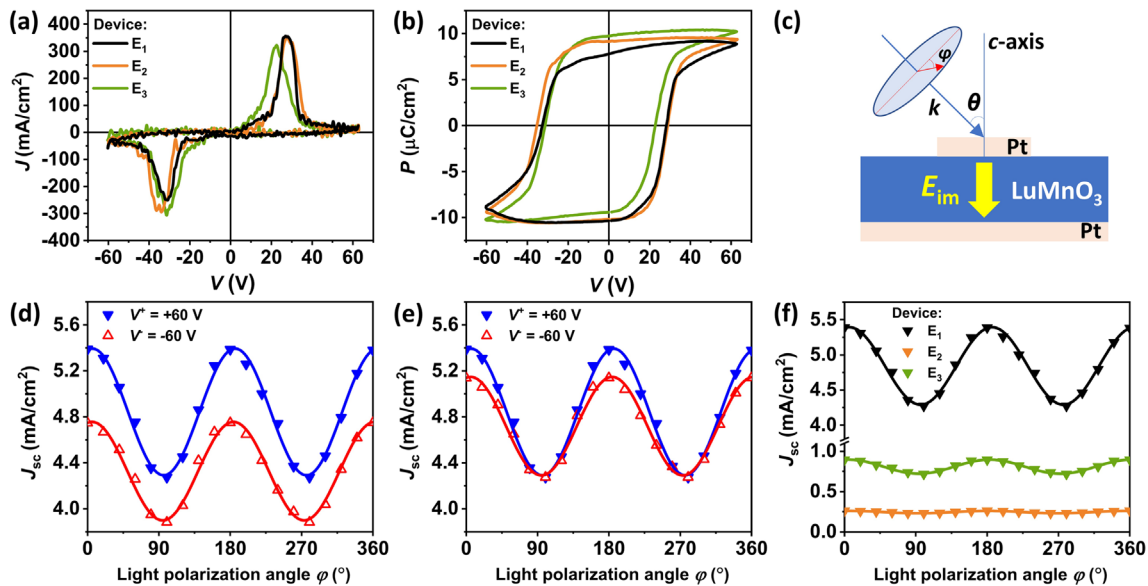


FIG. 1. (a) I - V curves and (b) corresponding polarization $P(V)$ loops collected using the Dielectric Leakage Current Compensation (DLCC) mode at 1 kHz, in capacitors E_{1,2,3} (crystal-I). (c) Sketch of the Pt/LMO/Pt sample, the illumination geometry, and the direction of the imprint field. (d) Dependence of the J_{sc} on the light polarization angle φ and on the sign of the prepoling voltage $V^{+/-}$ (crystal-I). (e) Data from (d) vertically shifted to emphasize the dependence of the amplitude of oscillations on $V^{+/-}$. (f) J_{sc} measured after V^+ , in capacitors E_{1,2,3} (crystal-I). In (d)–(f), solid lines are fits using Eq. (1) to experimental data (symbols).

back-switching time. To get information on the dynamics of the back-switching process, we have recorded polarization loops with a delay time $\tau_d = 1$ s, between polarization writing and reading as shown in Fig. 2.

The methodology to measure the remnant relaxation polarization $P_{r,rel}^-$ and $P_{r,rel}^+$ (retention) after saturation with V^- and V^+ is illustrated in Fig. 2(a). A $V(t)$ pulse sequence consisting of four bipolar triangular excitation signals (1 and 2, and 3 and 4) is applied to Pt_{top} with a delay time τ_d (1 s) between them. $P_{r,rel}^-$ is the polarization value after 1 s delay of negative prepoling, determined from the $P(V)$ loop recorded during pulse 2. Similarly, $P_{r,rel}^+$ is the polarization after 1 s delay of positive prepoling, determined from the $P(V)$ loop recorded during pulse 4. Positive values of polarization correspond to polarization pointing down (toward Pt_{bot}) and negative for polarization pointing up (toward Pt_{top}). Similar information is extracted from positive-up-negative-down (PUND) measurements (supplementary material, S3).

Data for devices $E_{1,2,3}$ [Figs. 2(b)–2(d)] reveal that in all cases, $P_{r,rel}^-$ has the same sign as $P_{r,rel}^+$, implying that polarization written with V^- has switched back to downward within $\tau_d = 1$ s, mimicking $P_{r,rel}^+$. As expected, as E_{im} increases from E_1 to E_3 the polarization difference of $P_{r,rel}^+$ and $P_{r,rel}^-$ decreases. Additional experiments indicate that longer delay (up to 1000 s) does not reveal further switching back (see the supplementary material, S4). Therefore, when $J_{sc}(\varphi)$ is recorded, the polarization always points down irrespectively on the writing voltage, as dictated by E_{im} . Accordingly, $A_z(V^+) > A_z(V^-)$ and $B_z(V^+) > B_z(V^-)$, and J_{sc} is positive as observed.

Crosscheck experiments have been performed using crystal-II where the $P(V)$ loops indicate that E_{im} is pointing upward [Fig. 3(a)],

and consistently, back-switching favors upward $P_{r,rel}^-$ [Fig. 3(b)]. The $J_{sc}(\varphi)$ data [Figs. 3(c) and 3(d)] show that the impact of polarization is reversed compared to data of crystal-I (Fig. 1), that is, $A_z(V^-) > A_z(V^+)$ and $B_z(V^-) > B_z(V^+)$. The fact that here, J_{sc} is still positive also denotes the presence of additional terms, probably related to a diffusion term due to non-homogenous illumination and/or a non-switchable drift contribution due to a pinned electric field.

The $\delta P_{r,rel} = \left| \frac{P_{r,rel}^+ - P_{r,rel}^-}{2} \right|$ is the difference of polarization measured at remanence after writing with $V^{+/-}$. It is to be expected that any polarization contribution to A_z and B_z should be encapsulated by $\delta P_{r,rel}$. To assess this hypothesis, we plot in Fig. 4(a) the $\delta A_z = |A_z(P_{r,rel}^+) - A_z(P_{r,rel}^-)|$ vs $\delta P_{r,rel}$ collected from 20 capacitors (crystal-I), all having the same imprint sign. Data show that the contrast of amplitude (δA_z) of $J_{sc}(\varphi)$ oscillations increases when reducing the back-switching (larger $\delta P_{r,rel}$). A similar trend can be appreciated in Fig. 4(b) where $\delta B_z = |B_z(P_{r,rel}^+) - B_z(P_{r,rel}^-)|$ vs $\delta P_{r,rel}$ is plotted. In short, both A_z and B_z change when reversing the polarization, and the stronger the retention of the pre-polarized states (bigger $\delta P_{r,rel}$), the larger the contrasts in δA_z and δB_z .

Several mechanisms may contribute to the photocurrent as observed in h -LuMnO₃¹² and other materials.²⁹ As the background term B_z may contain all these contributions, the role of ferroelectric P on B_z is difficult to discern. In contrast, understanding the dependence of the amplitude of oscillations on P appears at first sight simpler. Indeed, A_z reflects the sensitivity of the photoresponse to light polarization, and it is expected to provide a genuine fingerprint of BPE

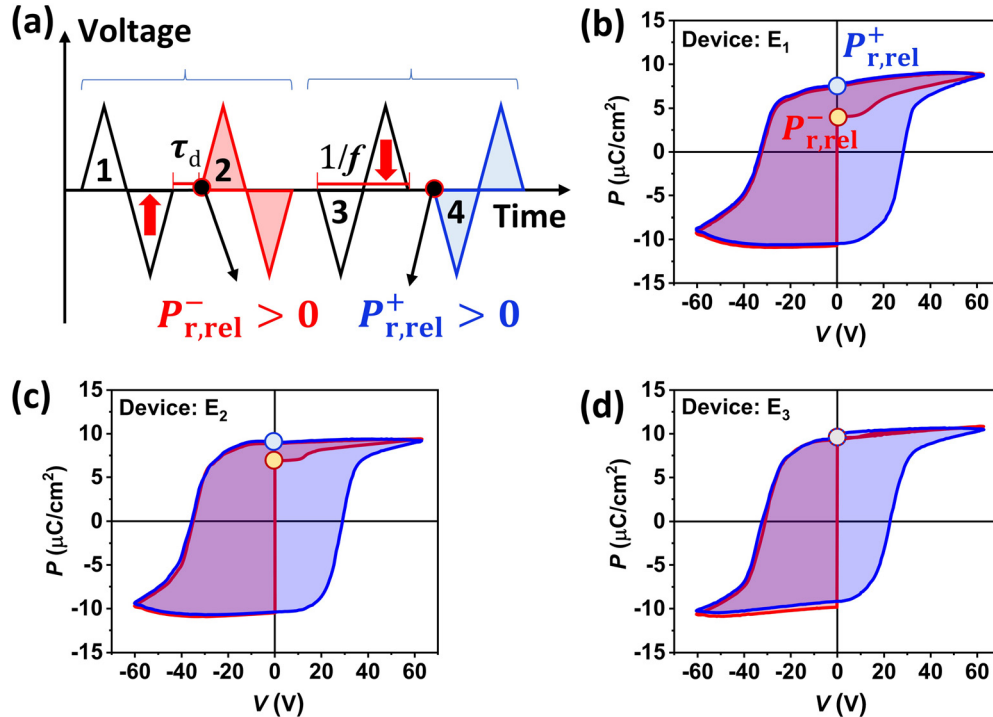


FIG. 2. (a) Voltage pulse trains used to determine the remnant polarization in $\tau_d = 1$ s, after V^- or V^+ writing pulses. (b)–(d) Polarization loops and retention in $\tau_d = 1$ s in capacitors $E_{1,2,3}$ (crystal-I), respectively.

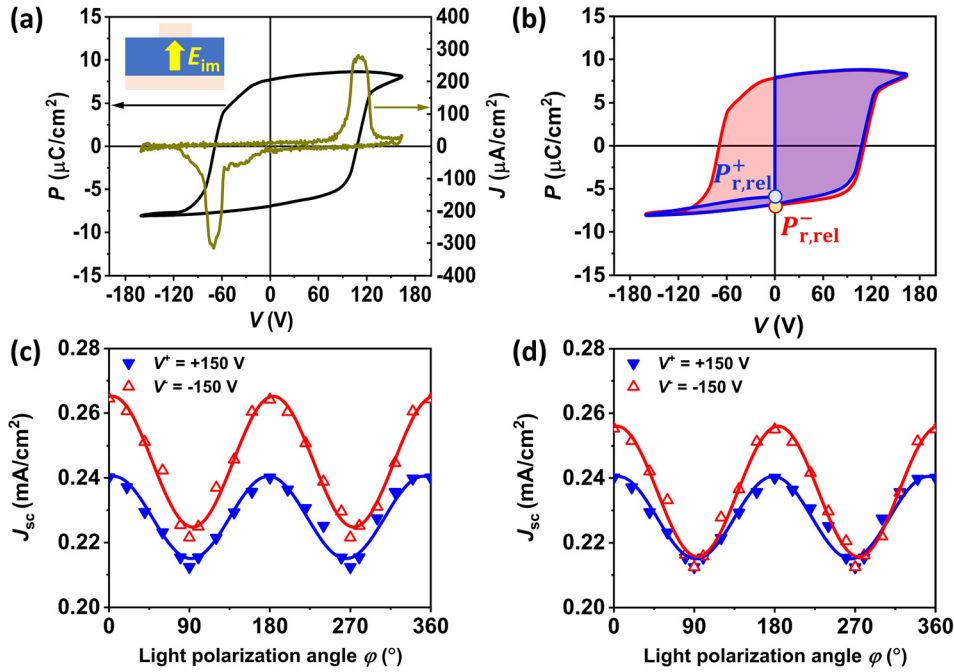


FIG. 3. (a) $I(V)$ and $P(V)$ loops and (b) retention in $\tau_d = 1$ s in crystal-II. (c) Raw $J_{sc}(\phi)$ and (d) the same data shifted to better visualize the change of amplitude; solid lines are fits using Eq. (1) to experimental data (symbols).

weighted by any Fresnel contribution. However, the observation that A_z depends on writing voltage (Figs. 1 and 3), implies that it is not simply determined by the symmetry of the crystal, but it is also affected by fine details of the polarization state of the sample when measurements are performed. As different capacitors on a given crystal have slightly different imprint fields [Figs. 1(a) and 1(b)], it is

expected that the polar state of the sample under the electrodes, when J_{sc} is measured at remanence, may differ from one capacitor to another. If so, the differences of A_z after $V^{+/-}$ writing, $\delta A_z = A_z(V^+) - A_z(V^-)$, could be a fingerprint and a reflection of the polarization retention, or in other words, a measure of the fraction of domains that may have switched back.

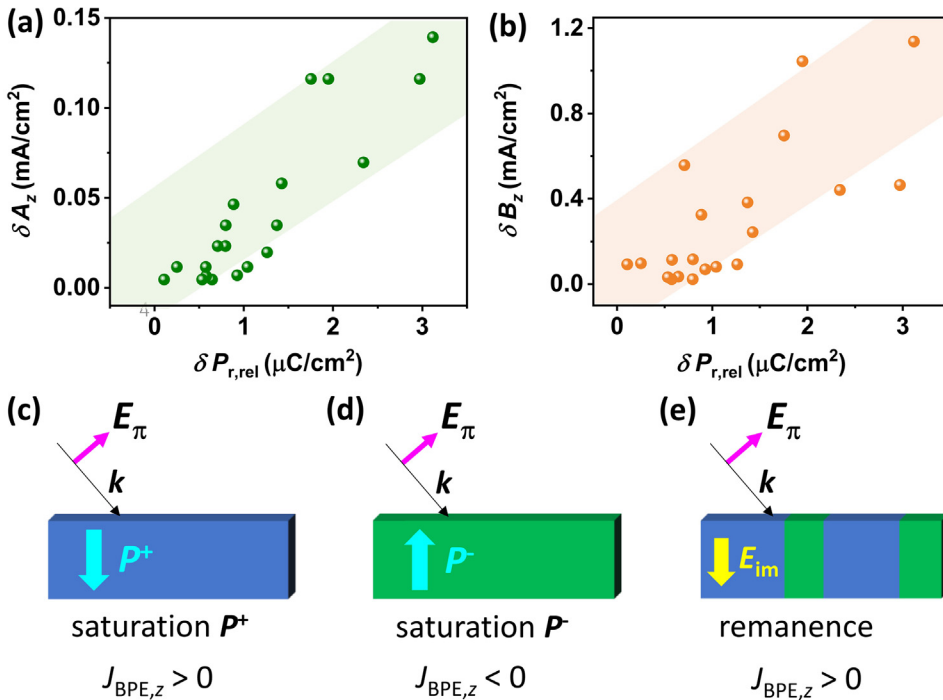


FIG. 4. Contrast of the oscillation (a) amplitudes (δA_z) and (b) backgrounds (δB_z) of $J_{sc}(\phi)$ vs the difference of remanent polarization ($\delta P_{r,rel}$) after $V^{+/-}$ writing, collected in 20 capacitors in crystal-I. Sketches represent the polarization at saturation of (c) P^+ (blue), (d) P^- (green) domains in the absence of back-switching, and (e) the polarization at remanence in the presence of back-switching, favoring P^+ state. Blue arrows indicate the polarization direction, the yellow arrow denotes the imprint direction, black arrows represent the propagation direction (k) of the light, and red arrows illustrate a π -polarized light (E_π).

To better understand the rationale behind, we recall that BPE photocurrent is given by

$$J_{\text{BPE},i}^+ = I_0 \alpha_{jk} G_{ijk}^+ e_j e_k, \quad (2)$$

where I_0 is the light intensity of a given wavelength, α_{jk} is the absorption coefficient, and G_{ijk} is the third rank Glass tensor.^{8,27} In Eq. (4), the suffixes (i, j, k) refer to (x, y, z) cartesian coordinates of the polarization components of the incoming light. We take the z -axis along the polar c -axis of h -LMO. As reported elsewhere,^{12,28} the oscillations of $J_{\text{BPE}}(\varphi)$ in h -LuMnO₃ of Fig. 1 can be well described by Eq. (2). The super index (+) emphasizes that the actual values of the tensor elements correspond to a net shift of positive ionic charges along the negative direction of z -axis, say P^+ , and under this circumstance, $J_{\text{BPE},z}^+$ is measured.

When polarization is fully reversed (P^-), preserving illumination conditions, Eq. (2) transforms to

$$J_{\text{BPE},i}^- = I_0 \alpha_{jk} G_{ijk}^- e_j e_k, \quad (3)$$

and $J_{\text{BPE},z}^-$ is measured. Polarization reversal in h -LuMnO₃ corresponds to a spatial inversion like a mirror ($m \perp c$) symmetry transformation. Therefore (see the [supplementary material](#), S1),

$$G_{ijk}^- = -G_{ijk}^+. \quad (4)$$

Equations (3) and (4) imply that under P reversal, $J_{\text{BPE},z}^-$ should display similar oscillations of the same amplitude but reversed sign than $J_{\text{BPE},z}^+$, that is, $J_{\text{sc}}(\varphi)$ should be phase-shifted by 90° . Under partial polarization back-switching, where the sample is in a mix state of polarization, the $J_{\text{BPE},z}$ would be the weighted sum of the $J_{\text{BPE},i}^{+/-}$ contributions.

Data of crystal-I [Figs. 1(d) and 1(e)] show that after $V^{+/-}$ writing, the current direction remains unperturbed. Only a relatively small change of amplitude ($\approx 5\%$) is observed. This implies that when J_{sc} is measured ($\tau_d > 1$ s), the polarization written with V^- has been partially switched back to P^+ state, in which case P_r^- is also downward but with a smaller magnitude than the fully stable P_r^+ (Fig. 2), thus the measured J_{sc}^- written with V^- keeps the same sign but smaller value than J_{sc}^+ written with V^+ . This process is sketched in Figs. 4(c)–4(e). It is expected to have opposite J_{sc} for downward and upward polarization states, respectively [Figs. 4(c) and 4(d)]. Instead, due to the presence of imprint, the final state can be a mixture of up and down domains impacting on the J_{sc} sign and magnitude. Thus, the presence of E_{im} is instrumental triggering the switching-back process and accounts for the observed dependence of $J_{\text{sc}}(\varphi)$ on the polarization state of crystal.

On the contrary, in crystal-II, where the upward E_{im} favors P^- , J_{sc}^+ is smaller than J_{sc}^- because the magnitude of real upward P_r^+ is smaller than fully switched P_r^- . However, the measured $J_{\text{sc}}^{+/-}$ is always positive (Fig. 3), and data show that the BPE-predicted phase shift of $J_{\text{sc}}(\varphi)$ compared with crystal-I is absent. Therefore, it follows that an additional contribution to $J_{\text{sc}}(\varphi)$ that does not change its sign under a mirror transformation should also coexist. As shown in BiFeO₃,³⁰ defect-related in-gap states in the ferroelectric may conspicuously affect the actual symmetry of G_{ijk} ⁷ while preserving the cosinusoidal $\cos 2\varphi$ dependence. The observation that the measured photocurrent differs among electrodes on the sample already indicates the importance of defects and/or impurities in the photovoltaic response, as already found in BiFeO₃.³¹ Finally, additional

contributions to $J_{\text{sc}}(\varphi)$ may originate from dichroism, as recently reported in BiFeO₃³² although earlier experiments indicated that this is not the case in LuMnO₃.²⁸ Even more, the polarization-dependent light transmittance (Fresnel) at the interfaces could impact both the BPE and drift or diffusion currents by adding a $\cos 2\varphi$ contribution to the measured $J_{\text{sc}}(\varphi)$ photovoltaic current. Its inspection is beyond the scope of this work.

Finally, we recall that the extraction of the Glass coefficients from the measured magnitude of $J_{\text{sc}}(\varphi)$ relies on the assumption that the measured photocurrent is dominated by bulk photovoltaic response, potentially affected by polarization back switching as demonstrated above. However, other effects such as drift photocurrent associated with band alignment at interfaces and/or diffusion photocurrent associated with photocarrier gradients contribute to the light-polarization insensitive background J_{sc} . Their presence, which precludes accurate extraction of some of the G_{ijk} elements, can be minimized by using optimized metallic electrodes and thin films.

In summary, the short circuit photocurrent J_{sc} in ferroelectric materials, measured at zero V -bias and, thus, at remanence, is largely affected by the polarization history of the sample and the presence of polarization back-switching and depoling processes. By measuring the dependence of $J_{\text{sc}}(\varphi)$ on the polarization of light, we have observed that the amplitude of $\cos 2\varphi$ oscillations depends on the polarization state of the ferroelectric at remanence, and thus, it is sensitive to the polarization back-switching. It follows that accurate extraction of the intrinsic Glass coefficients of the material, related to the amplitude of $J_{\text{sc}}(\varphi)$ oscillations, is challenging. As back-switching is typically more relevant in thin films, dedicated attention is required toward quantitative understanding of BPE. Moreover, data have been analyzed based on the assumption that BPE controls $J_{\text{sc}}(\varphi)$. However, it is worth noticing that similar $J_{\text{sc}}(\varphi)$ oscillations ($\approx \cos 2\varphi$) depending on the light polarization could be expected in the case of Fresnel controlled transmittance of π and σ light at top interfaces, and thus, a similar ferroelectric polarization dependent $J_{\text{sc}}(\varphi)$ could appear since the Schottky barriers at interfaces and depoling field are related to ferroelectric polarization. Disentangling both effects remains to be solved.

See the [supplementary material](#) for the Glass tensor (BPE) reversal upon switching the ferroelectric polarization, experimental methodology, PUND and retention measurements.

Financial support from the Spanish Ministry of Science and Innovation (10.13039/501100011033), through the Severo Ochoa FUNFUTURE (No. CEX2019-000917-S); the TED2021-130453B-C21 (AEI/FEDER, EU), PID2020-118479RB-I00 (AEI/FEDER, EU), and PID2019-107727RB-I00 (AEI/FEDER, EU) projects; and from CSIC through the i-LINK (No. LINKA20338) program is acknowledged. Project supported by a 2020 Leonardo Grant for Researchers and Cultural Creators, BBVA Foundation. Y.S. is financially supported by China Scholarship Council (CSC) through No. 201806410010. The work of Y.S. has been done as part of her Ph.D. program in Materials Science at Universitat Autònoma de Barcelona.

AUTHOR DECLARATIONS

Conflict of Interest

The authors have no conflicts to disclose.

Author Contributions

Yunwei Sheng: Data curation (lead); Formal analysis (lead); Investigation (lead); Writing – original draft (lead). **Ignasi Fina:** Conceptualization (equal); Writing – review & editing (equal). **Marin Gospodinov:** Methodology (equal). **Josep Fontcuberta:** Conceptualization (equal); Supervision (lead); Writing – review & editing (equal).

DATA AVAILABILITY

The data that support the findings of this study are available from the corresponding author upon reasonable request.

REFERENCES

- ¹V. M. Fridkin, *Crystallogr. Rep.* **46**, 654 (2001).
- ²V. M. Fridkin, *Photoferroelectrics* (Springer-Verlag, Berlin/Heidelberg/New York, 1979).
- ³A. M. Glass, D. von der Linde, D. H. Auston, and T. J. Negran, *J. Electron. Mater.* **4**, 915 (1975).
- ⁴V. M. Fridkin and B. N. Popov, *Sov. Phys. Usp.* **21**, 981 (1978).
- ⁵S. Y. Yang, J. Seidel, S. J. Byrnes, P. Shafer, C. H. Yang, M. D. Rossell, P. Yu, Y. H. Chu, J. F. Scott, J. W. Ager, L. W. Martin, and R. Ramesh, *Nat. Nanotechnol.* **5**, 143 (2010).
- ⁶M. Yang, A. Bhatnagar, and M. Alexe, *Adv. Electron. Mater.* **1**, 1500139 (2015).
- ⁷V. I. Belinicher and B. I. Sturman, *Sov. Phys. Usp.* **23**, 199 (1980).
- ⁸B. Sturman and V. M. Fridkin, *The Photovoltaic and Photorefractive Effects in Noncentrosymmetric Materials* (Gordon and Breach, Philadelphia, PA, 1992).
- ⁹L. Z. Tan, F. Zheng, S. M. Young, F. Wang, S. Liu, and A. M. Rappe, *npj Comput. Mater.* **2**, 16026 (2016).
- ¹⁰P. Würfel, *Physics of Solar Cells: From Basic Principles to Advanced Concepts* (John Wiley and Sons, 2005).
- ¹¹K. Buse, *Appl. Phys. B* **64**, 273 (1997).
- ¹²Y. Sheng, I. Fina, M. Gospodinov, and J. Fontcuberta, *Appl. Phys. Lett.* **118**, 232902 (2021).
- ¹³V. Koval, G. Viola, and Y. Tan, *Ferroelectric Materials-Synthesis and Characterization*, edited by A. P. Barranco (IntechOpen, 2015).
- ¹⁴A. Picinin, M. H. Lente, J. A. Eiras, and J. P. Rino, *Phys. Rev. B* **69**, 064117 (2004).
- ¹⁵Z. Tan, J. Tian, Z. Fan, Z. Lu, L. Zhang, D. Zheng, Y. Wang, D. Chen, M. Qin, M. Zeng, X. Lu, X. Gao, and J. Liu, *Appl. Phys. Lett.* **112**, 152905 (2018).
- ¹⁶V. I. Belinicher, *Sov. Phys. JETP* **48**(2), 322 (1978); available at <http://jetp.ras.ru/cgi-bin/e/index/e/48/2/p322?a=list>.
- ¹⁷C. Paillard, X. Bai, I. C. Infante, M. Guennou, G. Geneste, M. Alexe, J. Kreisel, and B. Dkhil, *Adv. Mater.* **28**, 5153 (2016).
- ¹⁸H. Han, S. Song, J. H. Lee, K. J. Kim, G. W. Kim, T. Park, and H. M. Jang, *Chem. Mater.* **27**, 7425 (2015).
- ¹⁹H. Han, D. Kim, S. Chae, J. Park, S. Y. Nam, M. Choi, K. Yong, H. J. Kim, J. Son, and H. M. Jang, *Nanoscale* **10**, 13261 (2018).
- ²⁰J. Yu, Y. Chen, S. Cheng, and Y. Lai, *Physica E* **49**, 92 (2013).
- ²¹M. Yang, D. J. Kim, and M. Alexe, *Science* **360**, 904 (2018).
- ²²H. L. Yakel, W. C. Koehler, E. F. Bertaut, and E. F. Forrat, *Acta Cryst.* **16**, 957 (1963).
- ²³A. M. Kalashnikova and R. V. Pisarev, *JETP Lett.* **78**, 143 (2003).
- ²⁴See M. N. Polyanskiy, <https://refractiveindex.info> for “Refractive index database” (last accessed 29 March 2022).
- ²⁵S. H. Kim, S. H. Lee, T. H. Kim, T. Zyung, Y. H. Jeong, and M. S. Jang, *Cryst. Res. Technol.* **35**, 19 (2000).
- ²⁶T. Yu, P. Gao, T. Wu, T. A. Tyson, and R. Lalancette, *Appl. Phys. Lett.* **102**(17), 172901 (2013).
- ²⁷W. Ji, K. Yao, and Y. C. Liang, *Phys. Rev. B* **84**, 094115 (2011).
- ²⁸Y. Sheng, I. Fina, M. Gospodinov, A. M. Schankler, A. M. Rappe, and J. Fontcuberta, *Phys. Rev. B* **104**, 184116 (2021).
- ²⁹M. Nakamura, S. Horiuchi, F. Kagawa, N. Ogawa, T. Kurumaji, Y. Tokura, and M. Kawasaki, *Nat. Commun.* **8**, 281 (2017).
- ³⁰M. Yang, Z. Luo, D. J. Kim, and M. Alexe, *Appl. Phys. Lett.* **110**, 183902 (2017).
- ³¹T. Choi, S. Lee, Y. J. Choi, V. Kiryukhin, and S. W. Cheong, *Science* **324**, 63 (2009).
- ³²A. Abdelsamie, L. You, L. Wang, S. Li, M. Gu, and J. Wang, *Phys. Rev. Appl.* **17**, 024047 (2022).